

# Relation between $2\Delta/T_c$ and nodes in Fe-based superconductors

Saurabh Maiti, Andrey V. Chubukov

Department of Physics, University of Wisconsin, Madison, Wisconsin 53706, USA

(Dated: April 14, 2022)

We analyze the interplay between the absence or presence of the nodes in the superconducting gap along electron Fermi surfaces (FSs) in Fe-pnictides, and  $2\Delta_h/T_c$  along hole FSs, measured by ARPES. We solve the set of coupled gap equations for 4-band and 5-band models of Fe-pnictides and relate the presence of the nodes to  $2\Delta_h/T_c$  being below a certain threshold. Using ARPES data for  $2\Delta_h/T_c$ , we find that optimally doped  $Ba_{1-x}K_xFe_2As_2$  and  $Ba(Fe_{1-x}Co_x)_2As_2$  and likely nodeless, but iso-valent  $BaFe_2(As_{1-x}P_x)_2$  likely has nodes.

*Introduction* The properties of Fe-based superconductors (FeSC) continue to attract interest in the condensed matter community. Amongst them, the pairing symmetry and the gap structure are the most debated topics. FeSCs are multi-orbital/multi-band quasi-2D systems, with 2 cylindrical hole pockets centered at  $(0,0)$ , and 2 cylindrical electron pockets at  $(\pi,0)$  and  $(0,\pi)$  in the unfolded Brillouin Zone(BZ), with one Fe-atom per unit cell. In some systems, there is an additional cylindrical hole pocket at  $(\pi,\pi)$ . This FS topology allows several different gap symmetries and structures:  $s^{++}$  and  $s^\pm$  s-wave states,  $d_{x^2-y^2}$  and  $d_{xy}$  states, etc.<sup>1-5</sup>. Most of the theoretical and experimental studies<sup>4,6-12</sup> favor a  $s^\pm$  state in which the gaps averaged along electron and hole pockets are of opposite sign. The  $s^\pm$  gap generally has some  $\pm \cos 2\theta$  variations along the two electron FSs and has accidental nodes when such a variation is large. Penetration depth and thermal conductivity data indicate that in some of the FeSCs the gap probably has no nodes<sup>13-15</sup>, while in the others accidental nodes are likely. The most compelling evidence for the nodes is for strongly doped  $Ba(Fe_{1-x}Co_x)_2As_2$ <sup>13,16</sup>,  $LaFeAsO_{1-x}F_x$ <sup>17</sup> and for iso-valent  $BaFe_2(As_{1-x}P_x)_2$ <sup>18</sup>.

The nodes in the gap can be directly probed by angle-resolved photoemission (ARPES). ARPES measures the gaps in the folded BZ, where the three hole FSs are all at  $(0,0)$  and the two electron FSs are both at  $(\pi,\pi)$ . At present, ARPES measurements distinguish between the gaps on the hole FSs, but cannot resolve the two gaps on the electron FSs (a possible exception is the hole-doped  $Ba_{1-x}K_xFe_2As_2$ <sup>19</sup>). The issue of the resolution is relevant because  $\cos 2\theta$  modulations of the gaps on the two electron FSs have  $\pi$  phase shift, and the convoluted (unresolved) gap remains a constant along the electron FS even if each of the two gaps has nodes.

Both conventional and laser ARPES measurements<sup>19-26</sup> have shown that the gaps on the hole FSs,  $\Delta_h$ , are weakly angle-dependent, but  $2\Delta_h/T_c$  differs from BCS value of 3.53 (Ref. 27). The issue we discuss in this communication is whether one can make a prediction, based on these measured  $2\Delta_h/T_c$ , about the presence or absence of the gap nodes on the electron FSs. We consider 4-pocket and 5 pocket models of FeSCs and argue that, if the largest  $2\Delta_h/T_c$  is below or above a threshold value (different for 4 and 5 pocket

models), the electron gaps either definitely have nodes, or definitely have no nodes, respectively. There is a “gray” area for  $2\Delta_h/T_c$  around the threshold, when the electron gap is either nodal or no-nodal, depending on parameters, but this gray area is rather narrow.

*Method* We ignore 3D effects, potential hybridization of the electron FSs in the folded BZ, and the difference between the gaps due to different densities of states  $N_F$  on different FSs, and focus on the two key features associated with multi-orbital/multi-band nature of FeSCs: the presence of multiple FS pockets and the angle dependencies of the interactions between low-energy fermions. The latter originates from the fact that orbital character of low-energy states varies along the FSs. In the band basis, this variation is passed onto the interactions which become angle dependent. We project the interactions onto  $s$ -wave channel, solve the coupled set of non-linear gap equations for the gaps along hole and electron FSs and relate  $2\Delta_h/T_c$  to the strength of the  $\cos 2\theta$  component of the electron gap.

We make several simplifying assumptions aiming to reduce the number of input parameters. First, we only keep the angular dependence of electron-hole interaction and approximate hole-hole and electron-electron interactions by constants. This is in line with the earlier study<sup>28</sup> which found that the structure of  $s^\pm$  gap is chiefly determined by the angle dependence of the electron-hole interaction  $u_{eh}(\theta)$ . Second, we factorize  $u_{eh}$  into an overall scale and an angular part in which we keep the leading  $2\theta$  harmonic:  $u_{eh} = u_{eh}(1 \pm 2\alpha \cos 2\theta)$  (for justification see Refs.<sup>28-30</sup>). Third, we take the ratios of different intra-band and inter-band hole-hole, electron-electron, and hole-electron interactions to be the values to which they flow under RG<sup>29</sup>. This leaves us with just three parameters: the magnitude of electron-hole interaction,  $u_{eh}$ , the factor  $\alpha$ , which measures the strength of its  $\cos 2\theta$  component, and the magnitude of intra-pocket hole-hole interaction  $u_{hh}$ . Other hole-hole and electron-electron interactions scale as  $u_{hh}$  with the prefactors (which are different in different models) set by the RG flow<sup>29</sup>. The overall magnitude of the interaction doesn't enter into  $2\Delta_h/T_c$ , hence the actual number of input parameters is two:  $\alpha$  and  $\beta \equiv u_{hh}/u_{eh}$ . We solve the non-linear gap equations in the two limits: when both hole FSs centered at  $(0,0)$  in the unfolded BZ are equal,

and when only one FS is present. This is done realizing that the actual case of the two non-equivalent hole FSs falls in between the two limits.

The gap structure for our interaction is specified by

$$\begin{aligned}\Delta_h^{(0,0)}(\mathbf{k}) &= \Delta_{h_1}, & \Delta_h^{(\pi,\pi)}(\mathbf{k}) &= \Delta_{h_2} \\ \Delta_e^{(\pi,0)}(\mathbf{k}), \Delta_e^{(0,\pi)}(\mathbf{k}) &= \Delta_{e_1} \pm \Delta_{e_2} \cos 2\theta,\end{aligned}\quad (1)$$

For brevity, we discuss our computational procedure only for the 4-pocket model with two identical hole FSs at  $(0,0)$ . The computations for other models are similar.

The set of coupled BCS-type equations at  $T=0$  is obtained by conventional means and reads:

$$\begin{aligned}\Delta_h &= -4\beta u_{he} \Delta_h \log \frac{2\Lambda}{|\Delta_h|} - \\ & 2u_{he} \int \frac{d\theta}{2\pi} (1 + 2\alpha \cos 2\theta) \Delta_e(\theta) \log \frac{2\Lambda}{|\Delta_e(\theta)|} \\ \Delta_{e_1} &= -4u_{he} \Delta_h \log \frac{2\Lambda}{|\Delta_h|} - 4\beta u_{he} \int \frac{d\theta}{2\pi} \Delta_e(\theta) \log \frac{2\Lambda}{|\Delta_e(\theta)|} \\ \Delta_{e_2} &= -8\alpha u_{he} \Delta_h \log \frac{2\Lambda}{|\Delta_h|}\end{aligned}\quad (2)$$

where  $\Delta_e(\theta) = \Delta_{e_1} + \Delta_{e_2} \cos 2\theta$  and  $\Lambda$  is the upper cutoff. We treat  $u_{he}$  as dimensionless, meaning that it is the product of the actual interaction and  $N_F$ .

The conventional route to find  $2\Delta/T_c$  is to compare these non-linear gap equations with the linear ones at  $T_c$ , solve for  $u_{he} \log \Lambda/T_c$ , substitute the result into the non-linear gap equation and obtain the closed-form equation for  $\tilde{\Delta}_i \equiv \frac{\gamma \Delta_i}{\pi T_c}$  ( $\log \gamma \approx 0.577$ ). For one-band BCS superconductor this yields  $\log \tilde{\Delta} = 0$ , i.e.,  $2\Delta/T_c = 2\pi/\gamma = 3.53$ . For a multi-band superconductor,  $2\Delta/T_c$  changes from 3.53 by two reasons: because hole and electron gaps are all different, and because the ratios between the gaps change by  $O(u_{he})$  in between  $T_c$  and  $T = 0$ . Accordingly, we introduce  $\Delta_{e_1} = \gamma_1 \Delta_h$ ,  $\Delta_{e_2} = \gamma_2 \Delta_h$  and write  $\gamma_1 = \gamma_1^o + u_{he} \gamma_1^1$ ,  $\gamma_2 = \gamma_2^o + u_{he} \gamma_2^1$ , where  $\gamma_{1,2}^o$  are the values of  $\gamma_{1,2}$  at  $T_c$ . We re-express the linearized gap equations at  $T_c$  as equations on  $u_{he} \log \Lambda/T_c$  and  $\gamma_{1,2}^o$ :

$$\left[ \mathbf{1} + \begin{pmatrix} 4\beta & 2 & 2\alpha \\ 4 & 4\beta & 0 \\ 8\alpha & 0 & 0 \end{pmatrix} u_{he} L \right] \begin{bmatrix} 1 \\ \gamma_1^o \\ \gamma_2^o \end{bmatrix} = 0, \quad (3)$$

where  $L = \ln \frac{\gamma \Lambda}{\pi T_c}$ . We solve (3), substitute the solutions into (2), collect terms  $O(u_{he})$  and obtain the set of three equations on  $\tilde{\Delta}_h$ ,  $\gamma_1^1$ , and  $\gamma_2^1$ , with  $\beta$  and  $\alpha$  as parameters:

$$\begin{pmatrix} 1 & 2l & 2\alpha l \\ \gamma_1^o & 1 + 4\beta l & 0 \\ \gamma_2^o & 0 & 1 \end{pmatrix} \begin{pmatrix} a \log \tilde{\Delta}_h \\ \gamma_1^1 \\ \gamma_2^1 \end{pmatrix} = - \begin{pmatrix} 2\chi_1 \\ 4\beta \chi_2 \\ 0 \end{pmatrix} \quad (4)$$

where  $\gamma_1^o$  and  $\gamma_2^o$  are the solutions of (3) (also functions of  $\alpha$  and  $\beta$  only),  $a = -(8\alpha)/\gamma_2^o$ , and

$$\begin{aligned}\chi_1 &= \int \frac{d\theta}{2\pi} (1 + 2\alpha \cos 2\theta) (\gamma_1^o + \gamma_2^o \cos 2\theta) L_\gamma \\ \chi_2 &= \int \frac{d\theta}{2\pi} (\gamma_1^o + \gamma_2^o \cos 2\theta) L_\gamma, \quad L_\gamma = \log \frac{1}{|\gamma_1^o + \gamma_2^o \cos 2\theta|},\end{aligned}$$

Solving this set we obtain  $\tilde{\Delta}_h$  and  $r \equiv |\Delta_{e_2}/\Delta_{e_1}| = \gamma_1/\gamma_2 \approx \gamma_1^o/\gamma_2^o$  as functions of  $\alpha$  and  $\beta$ . Comparing the two functions, we identify the  $\tilde{\Delta}_h$  for which  $r > 1$ , i.e., the gap along the electron FS has nodes.

*Results* In Fig. 1a we show  $\tilde{\Delta}_h$  for different  $\alpha$  and  $\beta$  compared to BCS value. The black line separates the regions of nodal and no-nodal gap ( $r > 1$  and  $r < 1$ , respectively). The nodal region corresponds to larger values of  $\alpha$  (larger angular dependence of the interaction) and larger  $\beta$  (larger intra-band repulsion). There is a critical value  $\beta_{critical} = 1/\sqrt{2}$  beyond which the gap remains nodal even when  $\alpha$  is infinitesimally small<sup>30</sup>. In Fig. 1b we take the slices of Fig. 1a and show the trajectories of  $\tilde{\Delta}_h$  for fixed values of  $r$  (for every given  $\beta$ , different  $r$  correspond to different values of  $\alpha$ ). We clearly see that there is a correlation between the magnitude of  $\tilde{\Delta}_h$  and whether the gap along electron FS is nodal or has no nodes. Namely, for  $\tilde{\Delta}_h$  above 0.73 the gap has no nodes, and for  $\tilde{\Delta}_h$  below 0.63, the gap has nodes, no matter what  $\alpha$  is. There is a ‘‘gray area’’ between 0.63 and 0.73 marked by dashed lines in the figure. For  $\tilde{\Delta}_h$  in this area, the gap is either nodal or no-nodal, depending on  $\alpha$ .

We found similar behavior for all cases that we studied. Namely, for  $\tilde{\Delta}_h$  above some threshold correspond the gap along the electron FSs has no nodes, for  $\tilde{\Delta}_h$  below some other threshold electronic gaps have nodes, and there is some relatively narrow ‘‘gray area’’ in between the thresholds. In Tab. I we summarize the main results for 4 pocket and 5 pocket models with either two equivalent hole FSs at  $(0,0)$  or only one hole FSs at  $(0,0)$ . These choices are dictated by our desire to minimize the number of input parameters and at the same time to understand a generic case of two non-equivalent hole FSs at  $(0,0)$ , which should be in between the two limits.

TABLE I: Table summarizing the main results for (a) 4 pocket model with 2 hole FSs at  $(0,0)$ , (b) 4 pocket model with 1 hole FS at  $(0,0)$ , (c) 5 pocket model with 2 hole FSs at  $(0,0)$ , and (d) 5 pocket model with 1 hole FSs at  $(0,0)$ .  $\Delta_h$  corresponds to the largest hole gap in each model. The ‘gray area’ values are relative to the BCS value of 3.53.  $2\Delta_h/T_c$  (also relative to the BCS value) and  $\Delta_{e_1}/\Delta_h$  are listed for  $\alpha \rightarrow 0, \beta \rightarrow 0$ .

	$\Delta_{e_1}/\Delta_h$	$\frac{2\Delta_h}{T_c}/3.53$	Gray area	$\beta_{critical}$
(a)	$-\sqrt{2}$	$2^{-1/4}$	0.63 – 0.73	$1/\sqrt{2}$
(b)	$-1/\sqrt{2}$	$2^{1/4}$	0.94 – 1.04	$\sqrt{2}$
(c)	-1	$2^{1/4}$	0.84 – 1.04	0.5
(d)	-1	1	0.78 – 0.87	1

*Comparison with experiments* A summary of the results is pictorially presented in ‘structure strips’ in Fig. 2, where for each case we show  $\tilde{\Delta}_h$  and its partition into the nodal, nodeless and the gray area. We keep the upper boundary open because strong coupling effects are known to increase the value of  $\tilde{\Delta}_h$ <sup>31</sup>. The symbols represent the ARPES data for the gaps along the hole FSs. Since our objective is to set an upper bound on  $\tilde{\Delta}_h$  for

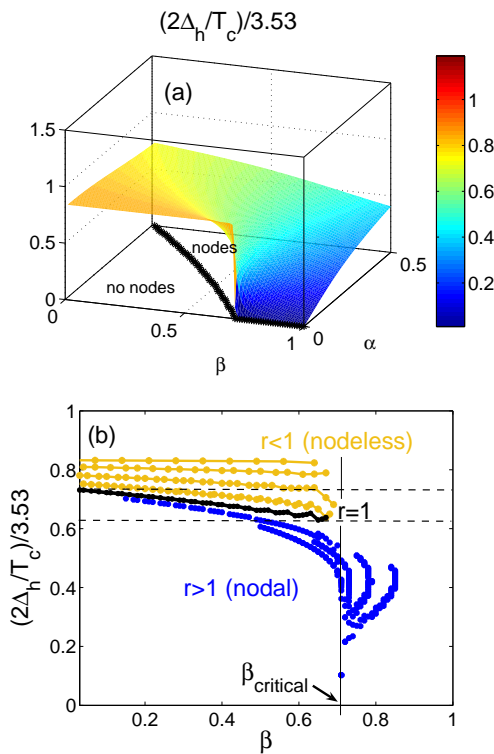


FIG. 1: (color online)  $2\Delta_h/T_c$  for the gap on one of the two identical hole pockets at  $(0,0)$  in the 4-pocket model. (a)  $2\Delta_h/T_c$  as a function of  $\alpha$  and  $\beta$ . The black line separates the nodal and nodeless regions. The colors indicate the gap magnitudes relative to the BCS value of 3.53. (b)  $2\Delta_h/T_c$  (relative to the BCS value) vs  $\beta$  for different values of  $r$ .  $r > 1$  (blue) are nodal lines,  $r < 1$  (yellow) are nodeless lines and  $r = 1$  (black) is the boundary line. The dashed lines indicate the boundaries of the ‘gray area’ (see text). Outside of gray area the gap either definitely has nodes or is definitely non-nodal.

nodal behavior, we compare the largest of the hole gaps from the theory to the largest hole gap observed in the experiments. The symbols above the line should be compared with the 4-pocket models and those below the line with the 5-pocket models.

For electron-doped 122 material  $Ba(Fe_{1-x}Co_x)_2As_2$ , both theory and experiment indicate that there are 2 hole and two electron pockets. ARPES result suggests<sup>24</sup> that one hole pocket is near-nested with electron pockets, while other is not. From our perspective, this should be close to our case of one hole and two electron pockets. We see that the measured  $\tilde{\Delta}_h$  near optimal doping sits well in the nodeless regime. This is consistent with specific heat and thermal conductivity data, which indicate that the gap in optimally doped  $Ba(Fe_{1-x}Co_x)_2As_2$  has no nodes<sup>13,32</sup>.

A similar situation holds for electron doped 1111 material  $NdFeAsO_{0.9}F_{0.1}$ . The measured  $\Delta_h$  is around  $15meV$ <sup>20</sup> for high  $T_c \approx 53K$ , which yields  $2\Delta_h/T_c \approx 6.57$ , well into the nodeless region. The no-nodal gap in high  $T_c$  1111 materials is consistent with penetration

depth measurements<sup>33</sup> assuming that inter-pocket impurity scattering is relevant<sup>34</sup>.

For 111 LiFeAs, which has 2 hole and 2 electron FSs, ARPES results<sup>25,26</sup> suggests that the measured  $\tilde{\Delta}_h$  is either in the nodeless region or near the upper boundary of gray area, suggesting that the full gap has no nodes, if, indeed LiFeAs is an  $s^\pm$  superconductor (see Ref. 35). The no-nodal electron gap is consistent with penetration depth and specific heat experiments<sup>15,26</sup> which clearly show exponential behavior at low  $T$ .

For hole-doped 122 material  $Ba_{1-x}K_xFe_2As_2$ , ARPES data show three hole FSs, consistent with the fact that these are hole-doped materials. The ARPES data for  $\tilde{\Delta}_h$  vary. The data by Nakayama *et al.*<sup>19</sup> show that the highest  $\tilde{\Delta}_h$  is rather large (about twice BCS value), which places this material deep into the nodeless region, where the gap along electron FSs is almost angle-independent. There is no evidence of nodes in this material from other measurements.<sup>36</sup>

Finally, for iso-valent doping in 122  $BaFe_2(As_{1-x}P_x)_2$ , recent laser ARPES measurements<sup>22</sup> detected three near-equivalent and near-isotropic hole gaps with  $\tilde{\Delta}_h \sim 0.85$ . This places the material near the lower boundary of the gray area (see Fig.2c), i.e., from our analysis, the measured  $\tilde{\Delta}_h$  implies that there must be nodes along the electron FSs. This is in line with thermal conductivity and penetration depth measurements, which show behavior consistent with the nodes in  $BaFe_2(As_{1-x}P_x)_2$ <sup>18</sup>. We caution, however, that the same laser ARPES study<sup>22</sup> reported  $\tilde{\Delta}_h \approx 0.52$  in  $Ba_{1-x}K_xFe_2As_2$ , much smaller than other ARPES measurements. That value would imply the nodes in  $Ba_{1-x}K_xFe_2As_2$ , in variance with what is known for this system.

**Conclusions** The purpose of his work was to investigate whether one can predict, based on the measured  $2\Delta_h/T_c$  along the hole FSs, whether or not the gaps on the electron FSs in FeSCs have nodes. The hole gaps have been measured by ARPES, but for most systems, ARPES measurements of the electron gaps separately on each of the two electron FSs are lacking. This issue is particularly relevant for systems like  $BaFe_2(As_{1-x}P_x)_2$ , in which penetration depth and thermal conductivity data show behavior consistent with the gap nodes.

We considered 4-pocket and 5-pocket models with angle-dependent interaction between hole and electron pockets and found that there is a direct correlation between  $2\Delta_h/T_c$  on hole FSs and the strength of  $\cos 2\theta$  oscillating gap component on the electron FSs. If  $2\Delta_h/T_c$  is larger than a certain value, there are no nodes, if it is smaller, then there must be nodes. There is a rather narrow range of  $2\Delta_h/T_c$  near the boundary where the electron gap is either nodal or not depending on the strength of the  $\cos 2\theta$  component of the interaction.

Most of ARPES data for  $\Delta_h$  are for near-optimally doped  $NdFeAsO_{0.9}F_{0.1}$ ,  $Ba(Fe_{1-x}Co_x)_2As_2$ ,  $Ba_{1-x}K_xFe_2As_2$ , and  $LiFeAs$  yield  $2\Delta_h/T_c$  above the threshold, meaning that there should be no nodes along the electron FSs. This is consistent with the penetration

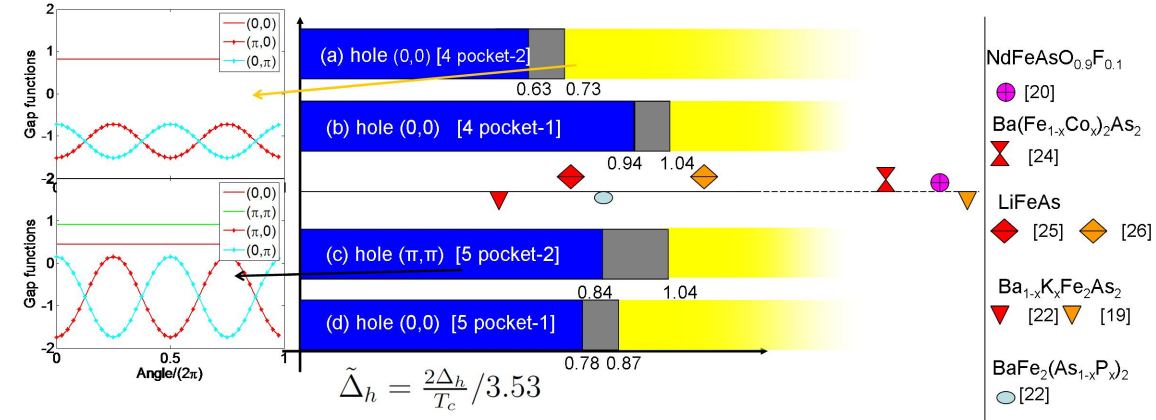


FIG. 2: (color online) Gap structure strips for (a) 4-pocket model with 2 identical hole FSs at (0, 0), (b) 4-pocket model with 1 hole FS at (0, 0), (c) 5-pocket model with 2 hole FSs at (0, 0) and (d) 5-pocket model with 1 hole FS at (0, 0). Each strip shows the regions of  $2\Delta_h/T_c$  for the largest hole gap in respective models where we find nodes (blue)/no-nodes (yellow) and the gray area (gray). The gaps are plotted in the left panel for one nodal and one non-nodal structure. The symbols are the ARPES values for  $2\Delta_h/T_c$  from various references. The symbols above the horizontal line should be compared with the 4-pocket models and those below the line with the 5-pocket models.

depth, thermal conductivity, and specific heat measurements in these materials. For P-doped  $\text{BaFe}_2(\text{As}_{1-x}\text{P}_x)_2$ ,  $2\Delta_h/T_c$  obtained by laser ARPES measurements is in the lower part of the gray area, meaning that the nodes on electron FSs are very likely. The detailed ARPES mea-

surements of the electron gaps separately on the two hole FSs are clearly called for.

We acknowledge helpful discussions with R. Fernandes, P. Hirschfeld, I. Eremin, Y. Matsuda, and M. Vavilov. This work was supported by NSF-DMR-0906953.

- <sup>1</sup> K. Kuroki, *et. al.*, Phys. Rev. Lett. **101**, 087004 (2008).
- <sup>2</sup> Q. Si and E. Abrahams, Phys. Rev. Lett. **101**, 076401 (2008).
- <sup>3</sup> P. A. Lee and X.-G. Wen, Phys. Rev. B **78**, 144517 (2008).
- <sup>4</sup> I.I. Mazin, *et. al.* Phys. Rev. Lett. **101**, 057003 (2008).
- <sup>5</sup> T. Saito, S. Onari, and H. Kontani, Phys. Rev. B **82**, 144510 (2010).
- <sup>6</sup> S. Graser, T. A. Maier, P. J. Hirschfeld, D. J. Scalapino, New J. Phys. **11**, 025016 (2009).
- <sup>7</sup> C. Platt, C. Honerkamp, and Werner Hanke, New J. Phys. **11**, 055058 (2009).
- <sup>8</sup> F. Wang, H. Zhai, D.-H. Lee, Phys. Rev. B **81**, 184512 (2010)
- <sup>9</sup> V. Cvetkovic and Z. Tesanovic, Phys. Rev. B **80**, 024512(2009).
- <sup>10</sup> A. V. Chubukov Physica C **469**, 640(2009), A. V. Chubukov, D. V. Efremov, and I. Eremin, Phys. Rev. B **78**, 134512(R)(2008).
- <sup>11</sup> R. M. Fernandes *et. al.*, Phys. Rev. B **81**, 140501(R) (2010).
- <sup>12</sup> A. D. Christianson *et. al.*, Nature **456**, 930(2008).
- <sup>13</sup> J.-Ph. Reid *et. al.*, Phys. Rev. B **82**, 064501 (2010); M.A. Tanatar *et. al.*, Phys. Rev. Lett. **104**, 067002 (2010).
- <sup>14</sup> R.R. Gordon *et. al.*, Phys. Rev. B **82**, 054507 (2010); L. Luan *et. al.*, Phys. Rev. Lett. **106**, 067001 (2011).
- <sup>15</sup> H. Kim, *et. al.*, arXiv:1008.3251 (2010).
- <sup>16</sup> G. Mu, *et. al.*, arXiv:1103.1300
- <sup>17</sup> J.D. Fletcher, *et. al.*, Phys. Rev. Lett. **102**, 147001 (2009).
- <sup>18</sup> K. Hashimoto, *et. al.*, Phys. Rev. B **81**, 220501(R) (2010).
- <sup>19</sup> K. Nakayama *et. al.*, Phys. Rev. B **83**, 020501 (2011); Y.-M. Xu, Nature Physics **7**, 198-202 (2011).
- <sup>20</sup> T. Kondo *et al*, Phys. Rev. Lett. **101**, 147003 (2008).
- <sup>21</sup> D. V. Evtushinsky *et. al.*, New J. Phys. **11**, 055069 (2009).
- <sup>22</sup> T. Shimojima *et. al.*, (unpublished)
- <sup>23</sup> Y. Sekiba *et. al.*, New J. Phys. **11**, 025020 (2009).
- <sup>24</sup> K. Terashima *et. al.*, Proceedings of the National Academy of Sciences of the USA (PNAS) **106**, 7330 (2009)
- <sup>25</sup> D. S. Inosov *et. al.*, Phys. Rev. Lett. **104**, 187001 (2010).
- <sup>26</sup> S.V. Borisenko *et. al.*, Phys. Rev. Lett. **105**, 067002 (2010)
- <sup>27</sup> D. S. Inosov *et. al.*, arXiv:1012.4041.
- <sup>28</sup> S.Maiti *et. al.*, arXiv:1104.1814.
- <sup>29</sup> S. Maiti and A.V. Chubukov, Phys. Rev. B **82**, 214515 (2010).
- <sup>30</sup> A. V. Chubukov, M. G. Vavilov and A. B. Vorontsov, Phys. Rev. B **80**, 140515(R) (2009).
- <sup>31</sup> See, e.g., D.J. Scalapino, Phys. Rep. **250**, 329 (1995).; F. Marsiglio and J.P. Carbotte, “Electron-Phonon Superconductivity”, in “The Physics of Conventional and Unconventional Superconductors”, edited by K.H. Bennemann and J.B. Ketterson, Springer-Verlag, 2006.
- <sup>32</sup> F. Hardy, *et. al.*, Euro Phys. Lett. **91**, 47008 (2010).
- <sup>33</sup> C. Martin *et. al.*, Phys. Rev. Lett. **102**, 247002 (2009).
- <sup>34</sup> A.B. Vorontsov, M.G. Vavilov, and A.V. Chubukov, Phys. Rev. B **79**, 140507(R) (2009).
- <sup>35</sup> B. Buechner *et. al.*, unpublished.
- <sup>36</sup> R. Khasanov, *et. al.*, Phys. Rev. Lett. **102**, 187005(2009).